scientific reports

Check for updates

OPEN

HSV-1 0ΔNLS vaccine elicits a robust B lymphocyte response and preserves vision without HSV-1 glycoprotein M or thymidine kinase recognition

Grzegorz B. Gmyrek[1], Amanda N. Berube[1], Virginie H. Sjoelund[2] & Daniel J. J. Carr[1,3]✉

Effective experimental prophylactic vaccines against viral pathogens such as herpes simplex virus type 1 (HSV-1) have been shown to protect the host through T and/or B lymphocyte-driven responses. Previously, we found a live-attenuated HSV-1 mutant, 0ΔNLS used as a prophylactic vaccine, provided significant protection against subsequent ocular HSV-1 challenge aligned with a robust neutralizing antibody response. Yet, how the virus mutant elicited the humoral immune response relative to parental virus was unknown. Herein, we present the characterization of B cell subsets in vaccinated mice at times after primary vaccination and following boost compared to the parental virus, termed GFP105. We found that 0ΔNLS-vaccinated mice possessed more CD4$^+$ follicular helper T (T_{FH}) cells, germinal B cells and class-switched B cells within the first 7 days post-vaccination. Moreover, 0ΔNLS vaccination resulted in an increase in plasmablasts and plasma cells expressing amino-acid transporter CD98 along with an elevated titer of HSV-1-specific antibody compared to GFP105-vaccinated animals. Furthermore, OΔNLS-vaccine-induced CD4$^+$ (T_{FH}) cells produced significantly more IL-21 compared to mice immunized with the parental HSV-1 strain. In contrast, there were no differences in the number of regulatory B cells comparing the two groups of immunized mice. In comparing sera recognition of HSV-1-encoded proteins, it was noted antiserum from GFP105-vaccinated mice immunoprecipitated HSV-1 thymidine kinase (TK) and glycoprotein M (gM) whereas sera from 0ΔNLS-immunized mice did not even though both groups of vaccinated mice displayed similar neutralizing antibody titers to HSV-1 and were highly resistant to ocular HSV-1 challenge. Collectively, the results suggest (1) the live-attenuated HSV-1 mutant 0ΔNLS elicits a robust B cell response that drives select B cell responses greater than the parental HSV-1 and (2) HSV-1 TK and gM are likely expendable components in efficacy of a humoral response to ocular HSV-1 infection.

Herpes simplex virus type 1 (HSV-1) is a highly transmissible pathogen that establishes a latent infection in which greater than 3.5 billion individuals under the age of 50 are infected worldwide many of which are asymptomatic or present with mild symptoms typically associated with oral mucocutaneous lesions[1]. More recently, HSV-1 has established itself as the leading cause of genital HSV infection in developed countries[2,3] and may contribute to the development or severity of Alzheimer's disease[4]. Whereas there are no licensed vaccines against HSV-1 to date, there are numerous experimental prophylactic vaccine candidates including live-attenuated, recombinant, subunit cocktail, and epitope-based vaccines[5–10]. Most, if not all, of these vaccines elicit some form of adaptive immune response with the generation of memory T and B lymphocytes. Moreover, the attenuated or recombinant virus vaccines are designed to reduce or eliminate the establishment of latency in comparison to their parental, wild type counterparts which, in turn, would reduce or eliminate the possibility of reactivation.

[1]Departments of Ophthalmology, The University of Oklahoma Health Sciences Center (OUHSC), 608 Stanton L. Young Blvd, DMEI PA415, Oklahoma City, OK 73104, USA. [2]Laboratory for Molecular Biology and Cytometry Research, The University of Oklahoma Health Sciences Center, Oklahoma City, OK 73104, USA. [3]Microbiology and Immunology, The University of Oklahoma Health Sciences Center, Oklahoma City, OK 73104, USA. ✉email: dan-carr@ouhsc.edu

The importance of the humoral response is unquestionable in defenses against viral infections including measles, rubella, and chicken pox viruses as resistance often depends on antibody levels[11]. B cells are central to the humoral response differentiating into antibody-secreting plasma cells. Indeed, in patients taking rituximab, an anti-CD20 monoclonal antibody which depletes peripheral B-cells and causes subsequent hypogammaglobulinemia, numerous viral infections are frequently reported[12,13]. Experimental studies have reported B-cell-deficient mice are less efficient in controlling HSV-1 infection with a higher incidence of encephalomyelitis and an increase in the establishment of viral latency[14–16]. This outcome may be influenced by the role of antigen presentation by B cells. Specifically, in HSV-1-infected B cell deficient mice, the number of $CD4^+$ T cells that differentiate into IFN-γ-expressing $CD4^+$ effector T cells are diminished whereas there are no significant changes in $CD8^+$ T cell or NK cell populations[17]. Thus, B lymphocytes are a critical cell population in antibody production and antigen presentation that along with T cell-driven antibody class switching and affinity maturation in the germinal centers[18,19] are instrumental in viral surveillance.

Draining lymph nodes are critical to the development of anti-viral immunity including T-dependent B cell class switching to IgG[20]. During the innate immune response to viral pathogens within the lymph node, type I IFNs are often expressed and facilitate the development of a Th1 response[21,22] and maintain lymphatic vessel expression for afferent delivery of antigen[23]. However, type I IFN can have detrimental outcomes to the B cell response as they can drive terminal B lymphocyte differentiation to short-lived plasma cells depleting the anti-viral B cell population through the combination of the local activation of myeloid cells and the expression of TNF-α[24]. Thus, a fine balance between the anti-viral innate defenses and B and T cell activation in response to virus infection must be maintained to optimize the adaptive immune response including the generation of memory T and B lymphocytes.

We have begun to characterize the host immune response to a live, attenuated HSV-1, termed HSV-1 0ΔNLS, used as a prophylactic vaccine against ocular HSV-1 challenge. This mutant virus lacks the nuclear localization signal of immediate early gene of infected cell protein 0 (ICP0) such that it is highly sensitive to the effects of type I IFN but remains highly immunogenic *in vivo*[25]. The efficacy has been linked to the humoral immune response as well as T cells that contribute to B cell help and $CD8^+$ effector T cell activation and function[5,26]. In the present study, the B lymphocyte profile in the draining lymph nodes of HSV-1 0ΔNLS vaccinated mice was conducted following the initial vaccine and boost. To determine if differences existed in the B cell response in vaccinating mice with an attenuated virus versus a fully competent virus, we compared the B cell profile of the HSV-1 0ΔNLS to the parental KOS counterpart, GFP105. Following the initial vaccination, there was a significant increase in the number of $CD4^+$ T follicular helper (T_{FH}) and B cell subsets residing in the spleen and draining (popliteal) lymph node of the 0ΔNLS vaccinated mice compared to the GFP105-vaccinated group. However, there was no change in antibody neutralization titers to HSV-1 following the initial vaccination or boost comparing the two vaccinated groups of mice. Likewise, there was no difference in efficacy in terms of preservation of the visual axis and lack of corneal pathology. However, two HSV-1 encoded proteins were not recognized by sera from 0ΔNLS vaccinated mice including glycoprotein M and thymidine kinase. Furthermore, there was a significant reduction in recognition of glycoprotein C by 0ΔNLS sera compared to sera from the parental virus vaccinated group in terms of peptide hits. Consequently, while mice vaccinated with the 0ΔNLS attenuated virus display equivalent resistance to subsequent ocular HSV-1 challenge compared with GFP105-vaccinated animals, there were noted differences in the humoral immune response such that we would conclude glycoprotein M and thymidine kinase are not necessary as antibody targets for prophylactic vaccine efficacy against ocular HSV-1 challenge.

Results

Primary Vaccination with HSV-1 0ΔNLS increases the number of T_{FH} cells and enhanced production of IL-21 that correlates with an increase in germinal center B cell formation. T helper (T_H) cells and dendritic cells play a critical role in the proliferation and differentiation of plasma cells and memory B cells initially taking place in distinct areas of the lymph nodes following tissue antigen (virus) exposure[27]. B cell proliferation within the follicles of the lymph node give rise to germinal centers, a specialized microanatomical region that provides an environment conducive to the selection of high-affinity antibody expressing B cells[18,28]. $CD4^+$ T follicular helper (T_{FH}) cells recruited to these sites through expression of CXCR5 facilitate germinal center (GC) B cell formation through interleukin (IL)-21 secretion[29,30]. To initiate our analysis of virus exposure to induction of B cell responses, we assessed whether vaccination of mice with HSV-1 0ΔNLS resulted in changes in $CD4^+$ T_{FH} cell defined as $CD45^+CD4^+PD1^+CXCR5^+Bcl\text{-}6^+$ (Fig. 1A) and GC B cell defined as $CD45^+CD19^+GL7^+CD95^+$ (Fig. 1B) numbers compared to mice vaccinated with parental HSV-1 (GFP105) in the draining (popliteal) lymph node (PLN) at days 7 and 21 and spleen at day 21 post footpad administration. The results showed significantly more $CD4^+$ T_{FH} cells and GC B cells in 0ΔNLS vaccinated mice compared to those immunized with the parental HSV-1 GFP105 at the day 7 time point in the PLN, and day 21 post immunization in the spleen (Fig. 1C, D, and Fig. 1E, F). These results paralleled frequency findings as well. Specifically, a greater percentage of $CD4^+$ T_{FH} and GC B cells were found in the PLN of 0ΔNLS vaccinated mice at day 7 ($13.09 \pm 0.85\%$ and $5.44 \pm 0.71\%$ respectively, $^*p < 0.05$) compared to that in the PLN of GFP105 immunized animals ($9.54 \pm 1.02\%$ and $3.46 \pm 0.3\%$). Likewise, a greater percentage of $CD4^+$ T_{FH} and GC B cells were found in the PLN of 0ΔNLS vaccinated mice at day 21 ($13.24 \pm 1.01\%$ and $2.71 \pm 0.31\%$ respectively, $^*p < 0.05$) compared to that in the PLN of GFP105 immunized animals ($9.56 \pm 0.97\%$ and $1.33 \pm 0.23\%$). Consistent with these findings, the percentage of $CD4^+$ T_{FH} cells expressing IL-21 from the PLN (Fig. 1G) was elevated in HSV-1 0ΔNLS vaccinated mice compared to mice immunized with HSV-1 GFP105 at day 7 post immunization (Fig. 1H). This result equated to nearly twice as many IL-21-expressing cells from the PLN of HSV-1 0ΔNLS vaccinated mice (58 ± 8) versus GFP105 immunized animals (31 ± 4). Likewise, IL-21 content in the PLN of HSV-1 0ΔNLS vaccinated animals was significantly higher compared to HSV-1 GFP105 immunized mice (Fig. 1I). No differences

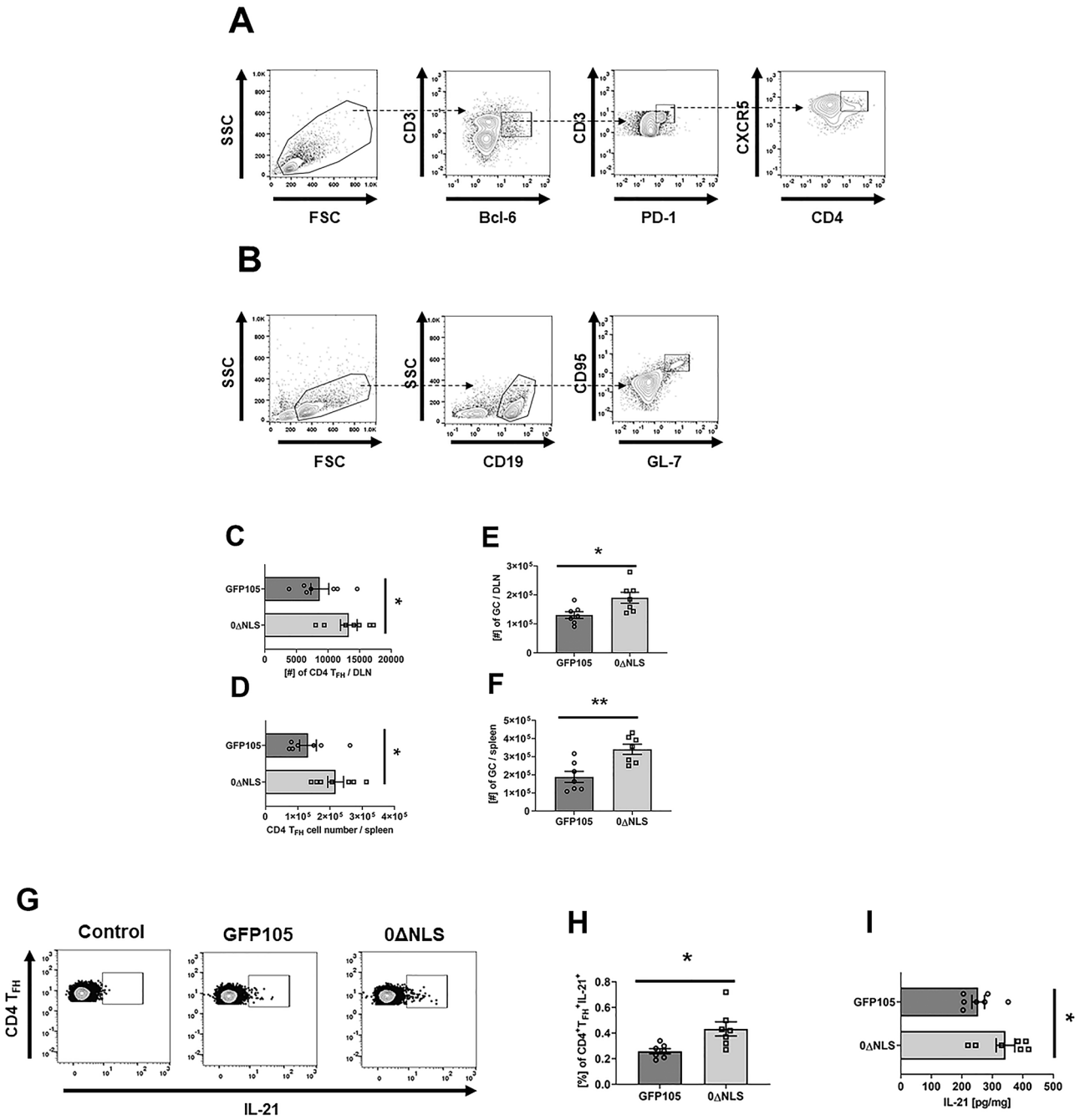

Figure 1. HSV-1 0ΔNLS vaccination induces more $CD4^+$ T_{FH} cells along with germinal center B cells. C57BL/6 mice (n = 6–7/group) were injected in the footpad with the HSV-1 parental (GFP105) or live-attenuated HSV-1 0ΔNLS at 10^5 plaque forming units in 10 µl PBS. At day 7 or day 21 post immunization, the PLN and spleen were harvested and $CD4^+$ T_{FH} cell and GC B cell numbers were assessed by flow cytometry. Panel A and B present gating strategy for discrimination of $CD4^+$ T_{FH} cells and GC B cells, respectively. Panel C shows the $CD4^+$ T_{FH} cell numbers found in the PLN at day 7 post-vaccination whereas panel D shows the CD4 + TFH cell numbers found in the spleen at day 21 post-vaccination. Panels E and F present the GC B cell numbers in the PLN at day 7 and in the spleen at day 21 post-vaccination, respectively. Panel G shows a representative flow cytometry profile of intracellular IL-21 cytokine staining in $CD4^+$ T_{FH} cells after stimulation with PMA and ionomycin. Panel H summarizes the results showing frequency of $CD4^+$ T_{FH} cells expressing IL-21. Panel I includes ELISA results quantifying the amount of IL-21 recovered in the PLN at day 7 post-vaccination normalized to tissue weight. The values are presented as mean ± SEM, $^{**}p < 0.01$ and $^{*}p < .05$ as determined by Student's *t*-test.

were noted in the total $CD4^+$ T cell count in the PLN or spleen comparing HSV-1 ΔNLS to GFP105 vaccinated animals (data not shown). Collectively, the results suggest HSV-1 ΔNLS promotes B cell expansion in the GC as a result of a specific increase in the number of IL-21 producing $CD4^+$ T_{FH} cells in the PLN.

Vaccination of mice with HSV-1 0ΔNLS results in an increase in the number of class-switched B cells associated with an increase in the titer of anti-HSV-1 antigen-specific IgG2b compared to HSV-1 GFP105 immunized animals. Production of high affinity antigen-specific immunoglobulin as a result of somatic hypermutation and class switching often leads to efficient eradication of pathogens through neutralization and/or antibody-dependent cellular cytotoxicity. As a means to further study the dynamics of B cell activation following exposure to HSV-1, we next investigated class-switching defined by $CD19^+IgD^-IgM^-$ B cells (Fig. 2A) in the PLN at day 7 or day 21 in the spleen post-vaccination. HSV-1 0ΔNLS vaccinated mice were found to possess significantly more $CD19^+IgD^-IgM^-$ B cells in the PLN and spleen at day 7 and day 21 post immunization, respectively (Fig. 2B, C). These results correlate with higher anti-HSV-1 IgG1 (Fig. 2D) and IgG2b (Fig. 2E) serum titers at day 21 post infection, although significance was noted only in case of anti-HSV-1 IgG2b (Fig. 2E). In contrast, there was no difference in the antibody neutralization titer to HSV-1 comparing mice vaccinated with 0ΔNLS versus parental GFP105 (Fig. 2F). Thus, whereas 0ΔNLS vaccinated mice display an elevation in class-switching that corresponds to increased anti-HSV-1 IgG2b titers, such results did not equate to an equivalent difference in antibody neutralization titers compared to GFP105 vaccinated mice suggesting a threshold in the level of anti-HSV-1 antibody titers has been reached in both vaccinated groups relative to virus neutralization. Nevertheless, the data does demonstrate an attenuated virus highly sensitive to type I IFN elicits a robust B cell antibody response that is equivalent to or greater than the non-attenuated parental virus when used as an immunogen to protect the host against ocular HSV-1 infection.

HSV-1 0ΔNLS vaccination induces higher number of plasmablasts and plasma cells expressing CD98. Antibody is produced by terminally differentiated B cells known as plasmablasts (PBs), which later give rise to plasma cells (PCs)[31]. The expression of the amino acid transporter CD98 has been shown to correlate with metabolic activity, longevity, antibody production, B cell proliferation and plasma cells formation[32–34]. In addition, the production of antibodies by long-lived plasma cells (LLPC) correlates with higher expression of CD98 as compared with short-lived plasma cells (SLPC)[34]. Given that the total number of PBs and PCs was not affected by vaccination (data not shown), we addressed how vaccination affect PBs and PCs in the context of their expression of CD98 at day 7 in the PLN and day 21 in the spleen post-vaccination. The expression of CD98 was found to be higher on PBs ($CD19^+CD138^+$, Fig. 3A) and PCs ($B220^{low}CD138^+$, Fig. 3B) in 0ΔNLS-vaccinated mice resulting in significantly more of these cells in the spleen at day 21 post-vaccination (Fig. 3C, D respectively) but not in the lymph node at day 7 post-vaccination (Fig. 3E, F respectively). These results were also found to be true assessing frequency with a significantly greater percentage of PCs in the spleen of 0ΔNLS-immunized mice at day 21 ($35.29 \pm 2.01\%$, $^*p < 0.05$) compared to that found in the GFP105 immunized mice ($19.66 \pm 1.64\%$) but not that found in the PLN of 0ΔNLS immunized mice at day 7 ($6.19 \pm 0.67\%$) compared to GFP105 vaccinated animals ($4.66 \pm 0.34\%$).

While most B cell subsets function are related to antibody production, cytokine secretion or antigen presentation, regulatory B cells (Breg) are known to possess immunosuppressive characteristics[35]. We characterized two Breg cell populations (Fig. 3G) that might have regulatory function including "classic" Breg cells (CD19+CD21+CD23+CD5+CD1d+) and a B cell population resembling marginal zone B cells (CD19+CD21+CD23-CD5+CD1d-)[36,37]. The data show both Breg cell subsets were modest in number in the draining lymph nodes at day 7 post-vaccination (Fig. 3H, I). However, by day 21 post-vaccination, both Breg cell populations were readily detectable in the spleen (Fig. 3J, K). Yet, at both time points evaluated there was no differences in the number of Breg cells residing in the PLN or spleen of GFP105 vs 0ΔNLS-vaccinated animals suggesting that changes in PB and PC numbers were not reflected by Breg cell numbers in either the spleen or PLN of vaccinated mice. In summary, HSV-1 0ΔNLS vaccine-induced animals develop a favorable B cell differentiation to PBs and PCs expressing CD98 over time evident by an increased number in the spleen. Such results are not apparent early on following vaccination in the PLN.

Class-switched and germinal center B cell numbers and IFN-γ-secreting, HSV-1 gB-specific $CD8^+$ T cell numbers remain elevated post-vaccination boost in the spleen of mice immunized with the 0ΔNLS vs GFP105 vaccine. Following primary vaccination, mice immunized with the 0ΔNLS vaccine showed an increase in the number of GC B cells and class-switched B cells in the spleen compared to animals immunized with GFP105 21 days post-vaccination. To determine if this relationship changed following re-exposure to antigen in the form of a vaccine boost, mice vaccinated with 0ΔNLS and GFP105 were boosted 21 days following the initial vaccination. Thirty days post-vaccine boost, the spleens of mice were evaluated for GC and class-switched B cell numbers. Consistent with the results following primary immunization, animals boosted with the 0ΔNLS vaccine possessed significantly more GC (Fig. 4A) and class-switched (Fig. 4B) B cells as well as IgG1-secreting (Fig. 4C) B cells compared with animals boosted with GFP105. However, there was no difference in neutralizing antibody titers of sera obtained from GFP105- versus 0ΔNLS-boosted animals (Fig. 4D).

Previously, we reported 0ΔNLS-vaccinated mice displayed more functional HSV-1 gB-specific $CD8^+$ T cells 7 days post-vaccination compared to mice immunized with GFP105[38]. Similar to the experimental design above, we wished to determine whether this relationship held following the booster immunization, mice vaccinated with GFP105 or 0ΔNLS were evaluated for IFN-γ-secreting, HSV-1 gB-specific $CD8^+$ T cells at 21 days post-primary immunization and 30 days post-boost. Similar to the results described for splenic B cells, there were nearly two

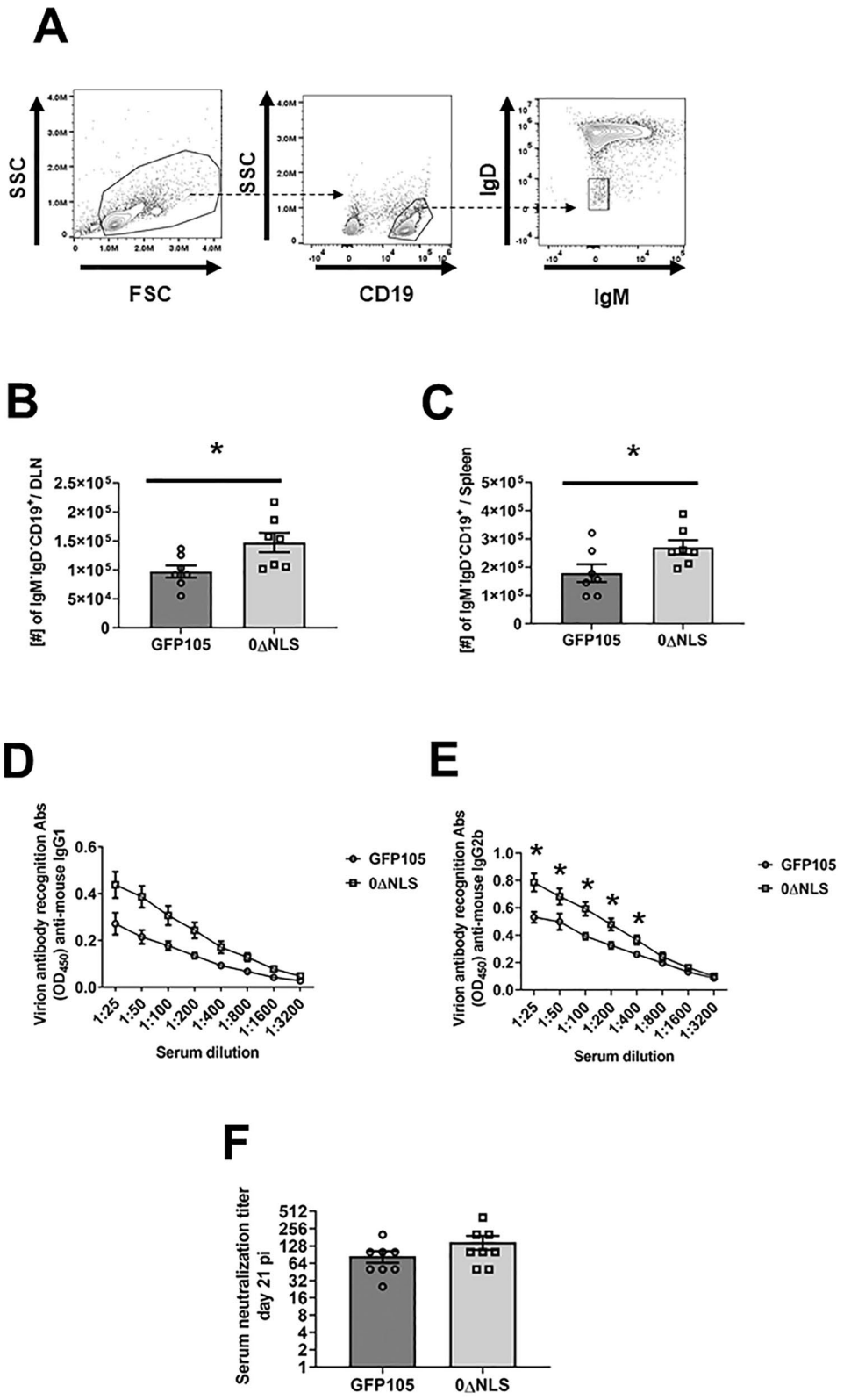

Figure 2. 0ΔNLS vaccination induces higher numbers of class-switch B cells along with an increase in HSV-1 IgG2b titers. C57BL/6 mice (n = 7–8/group) were injected in the footpad with the HSV-1 parental (GFP105) or live-attenuated HSV-1 0ΔNLS at 10^5 plaque forming units in 10 µl PBS. Mice were euthanized at day 7 and day 21 post-vaccination and the number of class-switched B cells was determined at day 7 in the PLN and day 21 in the spleen post-immunization. At day 21 post-vaccination, sera were obtained and stored at −80 °C until it was assayed for anti-HSV-1 antigen reactivity and virus neutralization. Panel A presents a gating strategy for class-switched B cells ($CD19^+IgM^-IgD^-$). Panels B and C present class-switched B cell numbers in the PLN and spleen of vaccinated animals, respectively. Panels D and E show anti-HSV-1 IgG1 and IgG2b immunoglobulin titers. Panel F presents antibody neutralization titers from sera of HSV-1 GFP105- and 0ΔNLS-vaccinated mice collected at day 21 post-immunization. The results are presented as the mean ± SEM, $^*p < .05$ as determined by Student's *t*-test.

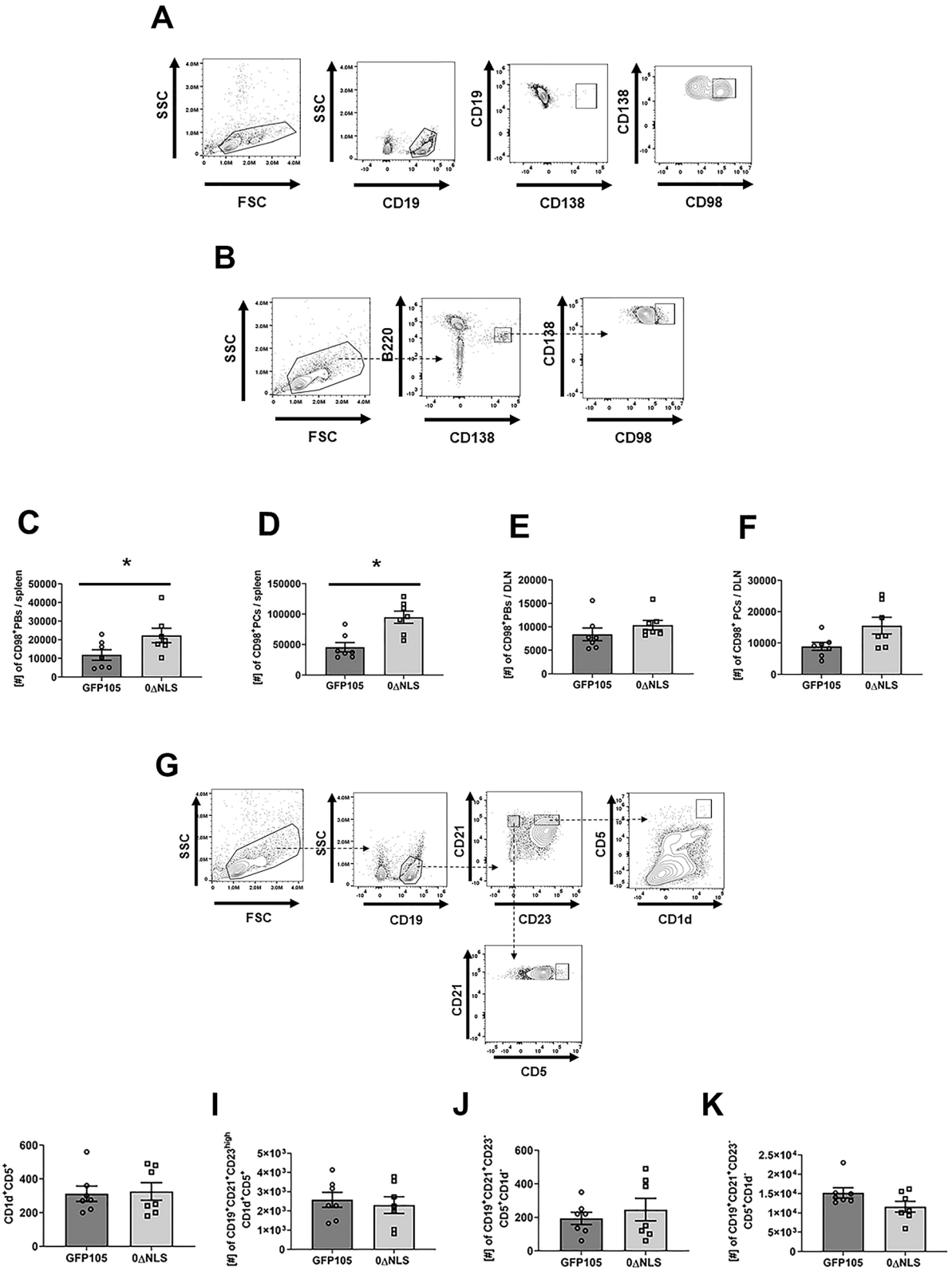
A
SSC
FSC
SSC
CD19
CD19
CD138
CD138
CD98
B
SSC
FSC
B220
CD138
CD138
CD98
C
[#] of CD98+PBs / spleen
GFP105
0ΔNLS
D
[#] of CD98+PCs / spleen
GFP105
0ΔNLS
E
[#] of CD98+PBs / DLN
GFP105
0ΔNLS
F
[#] of CD98+ PCs / DLN
GFP105
0ΔNLS
G
SSC
FSC
SSC
CD19
CD21
CD23
CD5
CD1d
CD21
CD5
H
[#] of CD19+CD21+CD23high CD1d+CD5+
GFP105
0ΔNLS
I
[#] of CD19+CD21+CD23high CD1d+CD5+
GFP105
0ΔNLS
J
[#] of CD19+CD21+CD23- CD5+CD1d+
GFP105
0ΔNLS
K
[#] of CD19+CD21+CD23- CD5+CD1d+
GFP105
0ΔNLS

◂**Figure 3.** 0ΔNLS vaccination induces a greater number of plasmablasts and plasma cells expressing CD98 but no change in B regulatory cells in the spleen. C57BL/6 mice (n = 7/group) were injected in the footpad with the HSV-1 parental (GFP105) or live-attenuated HSV-1 0ΔNLS at 10^5 plaque forming units (PFU) in 10 µl PBS. Mice were euthanized at day 7 and day 21 post-vaccination and the number of class-switched B cells was determined at day 7 in the PLN and day 21 in the spleen post-immunization. At day 7 and day 21 post-vaccination, the PLN and spleen were harvested and the number of plasmablasts (PBs) and plasma cells (PCs) expressing the CD98 marker were measured by flow cytometry. In addition, the number of $CD19^+CD21^+CD23^{high}CD5^+CD1d^{high}$ (regulatory B cell, Breg) along with marginal zone Breg cells ($CD19^+CD21^+CD23^-CD5^+CD1d^-$) were evaluated by flow cytometry as well. Panels A and B present a gating strategy for the evaluation of PBs expressing CD98 (CD19+CD138+CD98+) and PCs expressing CD98 (B220lowCD138+CD98+), respectively. Panels C and D show the number of PBs and PCs expressing CD98 in the spleen at day 21 post-vaccination respectively. Panel E and F show the number of PBs and PCs expressing CD98 in the PLN at day 7 post-vaccination, respectively. Panel G presents a gating strategy to discriminate Breg and marginal zone Breg cells. Panels H and I show the number of Breg cells in the popliteal lymph node at day 7 and in the spleen at day 21 post-vaccination, respectively. Panels J and K present the number of marginal zone Breg cells in the popliteal lymph node at day 7 and in the spleen at day 21 post-vaccination, respectively. The results are presented as the mean + SEM, $^*p < .05$ as determined by Student's t-test.

times as many IFN-γ-secreting $CD8^+$ T cells from the spleen of 0ΔNLS-vaccinated mice compared to those immunized with GFP105 at the 21-day time point (Fig. 4E). Whereas the re-exposure to antigen in the form of a boost expanded this population in both vaccinated groups of mice 30-days post-boost, a significant increase in the number of IFN-γ-secreting, HSV-1 gB-specific $CD8^+$ T cells from the 0ΔNLS-vaccinated animals was noted (Fig. 4E). Therefore, the effect of 0ΔNLS vaccination are not restricted to B cell populations but are found to influence functional $CD8^+$ T cells as well.

Visual axis remains intact in vaccinated mice following challenge with HSV-1. In mice, acute ocular HSV-1 infection often results in cornea pathology including denervation[39,40], opacity as a result of collagen fiber disruption[41], inflammatory hypoxia[42], local changes in substance P levels[43], and products of infiltrating leukocytes[44], hemangiogenesis[45], lymphangiogenesis[46], and edema[47] leading to blindness or significant vision loss[48]. In previous work, we found a clear association with vaccine efficacy and preservation of the visual axis in terms of architecture, cornea integrity, and vision performance[26]. Specifically, HSV-1-elicited cornea denervation parallels the loss of mechanosensory function during acute infection[40]. Likewise, corneal thickness and reduction in vision acuity have been noted following HSV-1 cornea infection[26]. To determine whether there was any difference in efficacy of vaccinated mice to ocular HSV-1 challenge, GFP105- and 0ΔNLS-vaccinated mice were infected with HSV-1 30 days post boost and evaluated for changes in the visual axis at 15 days post infection, a time when pathological changes within the cornea are evident and quantifiable[48]. We found no differences in the blink response associated with corneal denervation (Fig. 5A), edema (Fig. 5B), visual acuity (Fig. 5C), or neovascularization (Fig. 5D) comparing the vaccinated mice prior to and following infection. In the case of neovascularization (Fig. 5D), both GFP105- and 0ΔNLS-vaccinated animals showed no corneal neovascularization in comparison to HSV-1-infected naive, non-vaccinated mouse underscoring the robust nature of protection in generating a protective immune response using the attenuated HSV-1 0ΔNLS. Thus, GFP105- and 0ΔNLS-vaccinated animals show no loss in visual function or pathology suggesting equivalent degrees of efficacy against ocular HSV-1 infection.

Some HSV-1 encoded proteins are recognized by sera from GFP105- but not 0ΔNLS-vaccinated mice. Previous studies by our group and others have reported on the importance of humoral (antibody) immunity against HSV infection[26,49]. Although we found no difference in the neutralizing antibody titer comparing GFP105- to 0ΔNLS-vaccinated animals, there may be differences in the recognition pattern of antibodies to HSV-1-encoded proteins comparing the profiles generated from GFP105 and 0ΔNLS sera immunoprecipitated samples. Therefore, we utilized mass spectrometry to identify virus-encoded proteins recognized by antiserum from GFP105- and 0ΔNLS-vaccinated animals. The results show a total of 44 HSV-1-encoded proteins were identified from immunoprecipitated samples using GFP105 sera compared to 42 proteins from 0ΔNLS sera. Two proteins uniquely precipitated by GFP105 sera included unique long (UL)10/glycoprotein (g) M and UL23/thymidine kinase (TK) (Fig. 6). Furthermore, two proteins immunoprecipitated by the GFP105 sera were found to have significantly higher peptide hits compared to that immunoprecipitated by 0ΔNLS sera including UL50/dUTPase and UL44/gC (Fig. 6). No other HSV-1-encoded proteins identified by relative abundance of peptide hits were found to be different between GFP105 and 0ΔNLS immunoprecipitated samples (data not shown). Of note, antibody recognition of proteins previously found to correlate with preservation of the visual axis including UL19/virion protein (VP)5, UL29/infected cell protein (ICP)8, UL27/gB, UL40/ribonuclease reductase subunit (RR)2, unique short (Us)6/gD, Us8/gE, UL1/gL, UL48/VP16, and UL12/alkaline nuclease (AN)[50] were found to be recognized by antiserum from GFP105- and 0ΔNLS-vaccinated mice suggesting these proteins may be critical in immune recognition to control acute ocular HSV-1 infection. We interpret the results to also suggest HSV-1-encoded TK and/or gM are not critical viral proteins to mount an antibody response to since the lack of recognition by antiserum from 0ΔNLS-vaccinated mice did not lessen preservation of the visual axis.

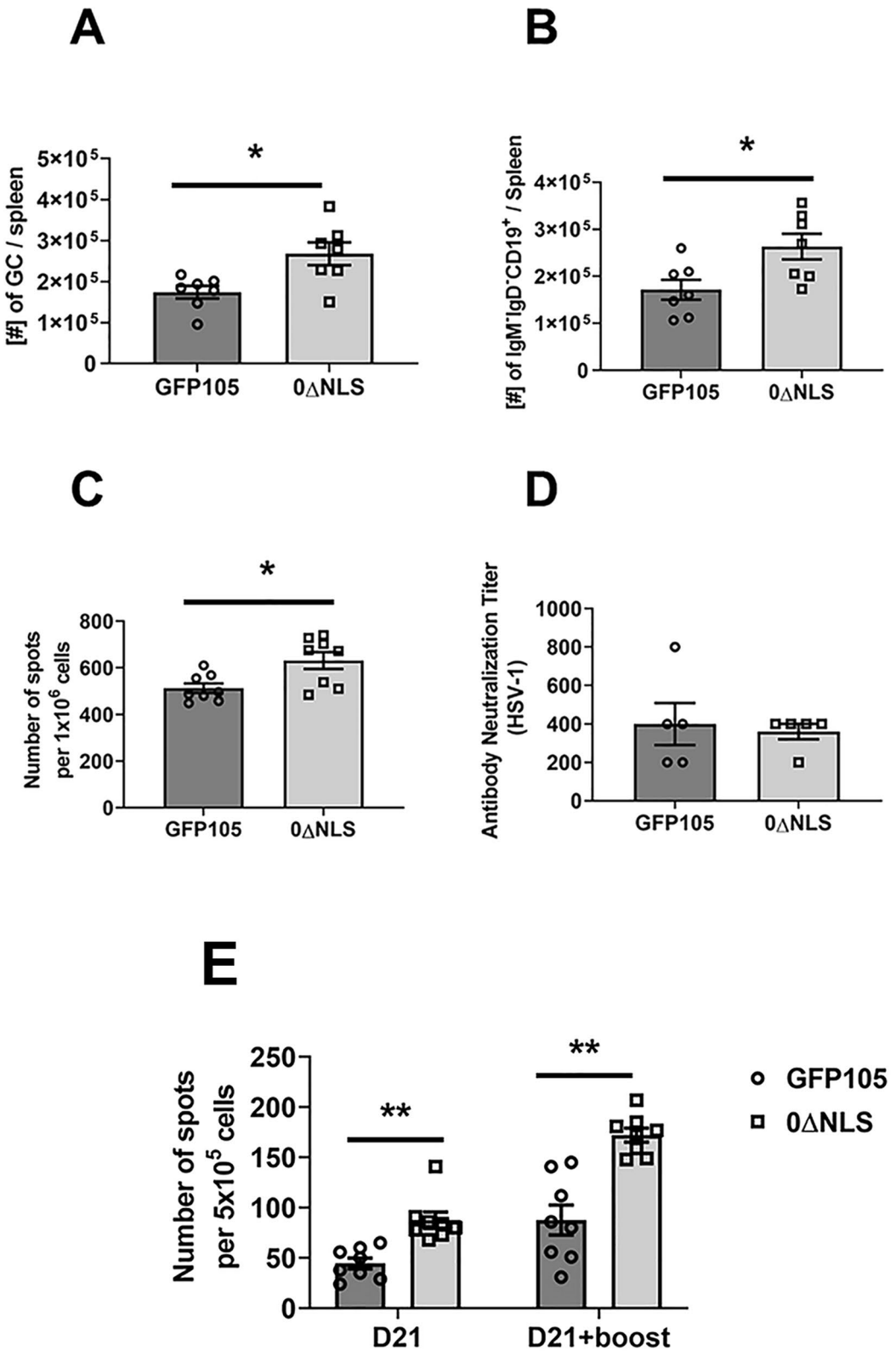

Figure 4. Primary immunization combined with boost vaccination results in an increase in the number of germinal center and isotype-switched B cells and IFN-γ-secreting, HSV-1 gB-specific $CD8^+$ T cells in 0ΔNLS vaccinated mice. C57BL/6 mice (n = 5–8/group) were injected in the footpad with the HSV-1 parental (GFP105) or live-attenuated HSV-1 0ΔNLS at 10^5 plaque forming units (PFU) in 10 µl PBS. At day 21 post immunization, the mice were boosted with the same amount of either parental or live-attenuated HSV-1 virus and left for 30 days. Thirty days after boosting, mice were exsanguinated to evaluate (**A**) germinal center (GC) B cell ($CD19^+GL\text{-}7^+CD95^+$) and (**B**) isotype-switched B cell ($CD19^+IgM^-IgD^-$) formation along with (**C**) analysis of the number of pre-activated B cells secreting IgG1 after polyclonal stimulation, and (**D**) HSV-1 neutralization titer from sera obtained from mice 30 days post-booster. (**E**) The spleens were removed and processed to single-cell suspensions in which 1×10^6 cells/well were stimulated overnight with gB peptide, SSIEFARL (10 µg/ml) to measure IFN-γ secreting $CD8^+$ T cells by ELISPOT assay. Bars represent the mean ± SEM, $^{**}p < .01$, $^{*}p < .05$ comparing the indicated groups as determined by Student's *t*-test.

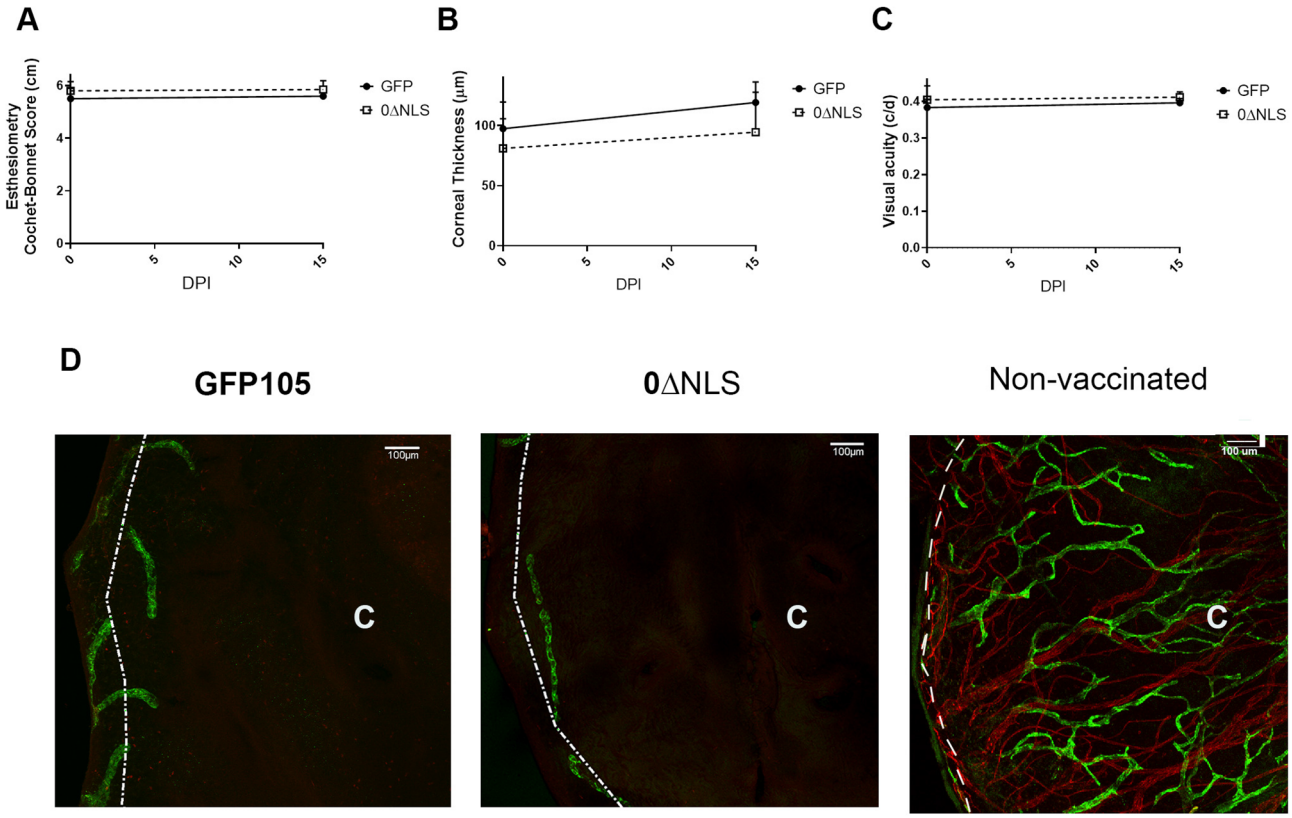

Figure 5. Visual axis is not compromised in vaccinated mice. C57BL/6 mice (n = 10/group) were injected in the footpad with the HSV-1 parental (GFP105) or live-attenuated HSV-1 0ΔNLS at 10^5 plaque forming units (PFU) in 10 µl PBS. At day 21 post immunization, the mice were boosted with the same amount of either parental or live-attenuated HSV-1 virus and left for 30 days. Thirty days after boosting, mice were evaluated for mechanosensory function, edema, and peripheral vision (day 0) prior to challenge with HSV-1 (10^4 PFU/cornea). At day 15 post infection, the mice were evaluated for (**A**) mechanosensory function measured by an esthesiometer, (**B**) cornea edema measured by optical coherence tomography and (**C**) visual acuity by optokinetic tracking. Mice were then exsanguinated and the corneas removed, processed, and stained for blood (red, $CD31^+$) and lymphatic (green, $Lyve\text{-}1^+$) vessels with images captured by confocal microscopy. A non-vaccinated mouse cornea stained in the same manner shows blood and lymphatic vessel genesis into the central cornea. The "C" indicates the location of the central cornea. The white dotted line depicts the limbus/cornea border. The scale bars are depicted at 100 µm.

Discussion

There are many extrinsic and intrinsic factors that influence B cell survival, proliferation, differentiation, isotype switching and immunoglobulin secretion[51–55]. Cytokines are one set of factors that have a critical role in the regulation of B cell activation. For example, IFN-γ induces B cell proliferation as well as increases in IgG2 production[56,57]. Type I IFN augments B cell activation as well as differentiation to antibody-secreting cells and B cell receptor sensitivity[58,59]. Still, another cytokine IL-12, has been shown to promote differentiation of naive B cells into plasma cells[60]. In a previous study, we reported following initial vaccination with HSV-1 0ΔNLS, an elevation in type I IFN and IL-12 production by cells was noted which drove an increase in IFN-γ-expressing $CD8^+$ T cells in comparison to mice vaccinated with GFP105[38]. Thus, using the same vaccination model, changes in B cell subset formation may be linked to an altered cytokine microenvironment.

$CD4^+$ T_{FH} cells play an important role in the regulation of T-cell dependent, B cell activation and differentiation. They are positioned within GC where they support the GC B cell activation, specifically B cell proliferation, class-switch recombination and differentiation of B cells into plasma cells[30,61,62]. In the present study, we report an increased number of $CD4^+$ T_{FH} cells along with increased secretion of IL-21 by these cells. The importance of IL-21 in the regulation of B cell function has been described using IL-21 receptor-deficient mice. These mice were found to possess a compromised humoral immune response to T cell-dependent antigens. Specifically, GC B cells were found to be severely impaired resulting in an attenuated B cell proliferation response with a deficiency in plasma cell differentiation[63–66]. Similar to the current results, it was reported vaccination with another live-attenuated HSV-1 virus termed VC2 resulted in increased proliferation of $CD4^+$ T_{FH} cells that correlated with robust antibody production and GC B cell activation[67]. Taken together, these studies underscore the strong influence of $CD4^+$ T_{FH} production of IL-21 on GC B cell responses relative to PB and PC numbers as well as increased anti-HSV-1 antibody levels. While the mechanism that drives enhanced GC B cell activation is currently unknown, it is tempting to speculate it may involve levels of lymphotoxin generated by localized T cells

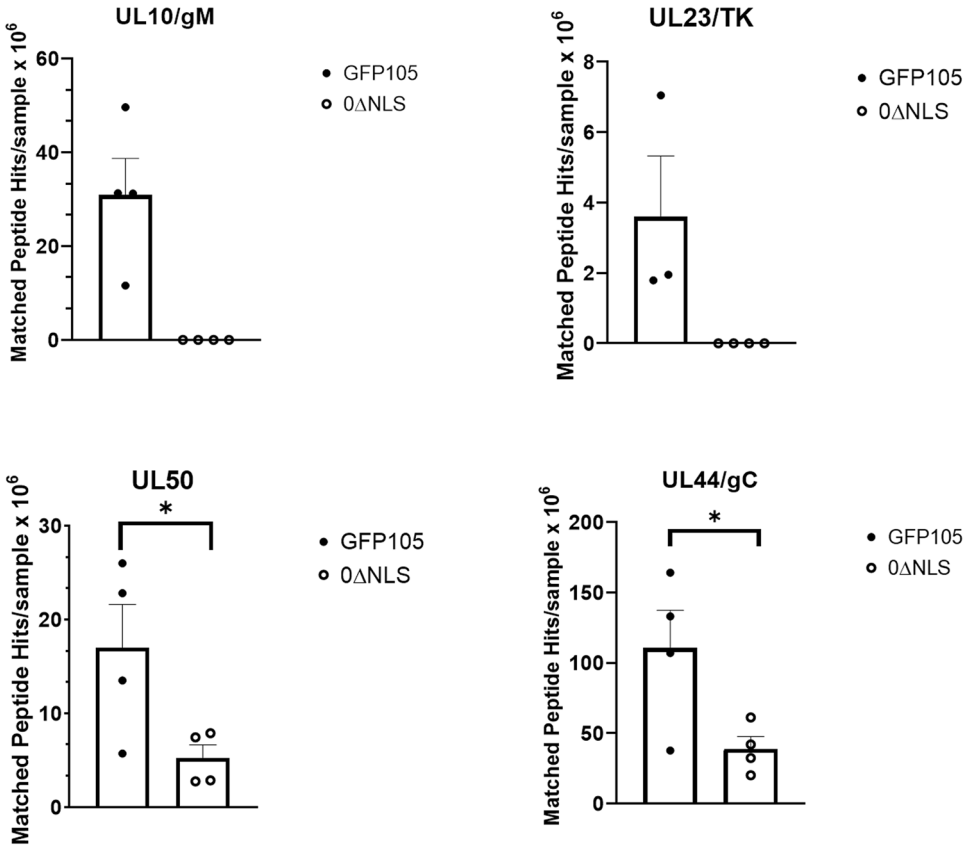

Figure 6. HSV-1 gM and TK are recognized by antiserum from GFP105- but not 0ΔNLS-vaccinated mice. Serum (n = 4 samples/group) from GFP105- and 0ΔNLS-vaccinated mice was used to immunoprecipitate virus-encoded proteins from HSV-1-infected Vero cell lysates. Precipitated proteins were analyzed by mass spectrometry. HSV-1 proteins were identified via cross-referencing derivative peptide ions with a reference sequence data base. The bars represent the mean matched peptide abundance/intensity per protein ± SEM, $^{*}p < .05$ comparing the two groups as determined by multiple t-test using the Holm-Sidak method.

as a previous study reported a loss in T_{FH} cells and impaired antibody response to HSV-1 using a lymphotoxin β receptor deficient mouse model[68].

Our previous studies described changes in cell metabolism might be linked to effector function of $CD8^{+}$ T cells. Relative to B lymphocytes, the activation and differentiation states of B cells may depend on their metabolism[69,70]. Long-lived plasma cells expressing amino-acid transporter CD98 utilize 90% of their cellular glucose not to generate ATP and metabolites but rather, for glycosylation of secreted antibodies[32]. The present study found mice vaccinated with 0ΔNLS possessed more PB and PC expressing CD98 in the spleen 3 weeks after primary vaccination in comparison to mice vaccinated with GFP105. Whether the 0ΔNLS vaccination altered cell metabolism in the naive B cells driving proliferation and differentiation is currently unknown. CD98 deficiency has been reported to reduce B cell proliferation, PC formation, and antibody production; however, B cell proliferation does not depend on amino-acid transport function but rather CD98 supports integrin-dependent proliferation of B cells[34]. Further studies are needed to reveal whether an interconnected network of genes and metabolic pathways correlate with PC function after vaccination with HSV-1 0ΔNLS.

In addition to characterizing the initial B cell response following vaccination with 0ΔNLS and GFP105, we also evaluated the response following vaccine boost 21 days post primary vaccination. Similar results in the B cell responses were noted. Furthermore, vaccinated mice retained and preserved their visual axis whether immunized with HSV-1 GFP105 or 0ΔNLS. These results are critical for two reasons: (1) the attenuated HSV-1 0ΔNLS elicits the same if not better humoral immune response as the fully virulent parental virus used as vaccines and (2) the immune response provides sufficient protection to retain the integrity and performance of the visual axis. Most experimental studies do not go into depth in terms of evaluating the cornea and how changes to its architecture may hinder the rodent's peripheral vision. Denervation of the cornea in response to HSV-1 infection is a common response in mice[39,40]. Likewise, inflammation of the cornea as a result of HSV-1 infection in experimental animal models often leads to edema and neovascularization[23,71]. The culmination of these and other events can lead to a loss of peripheral vision as measured by optomotor kinetic tracking or OKT[26]. In the current study, the evaluation of these parameters in comparing HSV-1 0ΔNLS to GFP105 demonstrates that the attenuated virus delivers the same degree of protection at a reduced risk of establishing latency compared to the parental virus[25]. Such results are consistent with equivalent neutralizing antibody titers to HSV-1 which we

have previously reported is an essential component of a protective immune response associated with the HSV-1 0ΔNLS vaccine[5]. However, upon evaluation of viral proteins recognized by antiserum from vaccinated animals, there were noted deficiencies in the recognition of some viral-encoded proteins in the 0ΔNLS-vaccinated group. Specifically, 0ΔNLS-induced antiserum did not immunoprecipitate HSV-1 gM or TK where sera from GFP105 immunized mice did. Moreover, recognition of HSV-1 UL50- and gC-encoded proteins based on peptide hits was reduced in the immunoprecipitated samples from 0ΔNLS sera pulldowns. However, other virus-encoded proteins previously found to correlate with vaccine efficacy including VP5, ICP8, gB, RR2, gD, gE, gL, VP16, and AN[50] were recognized by GFP105 and 0ΔNLS antiserum. Thus, we conclude these proteins are important in the recognition by antibody to suppress virus replication and spread from the eye to the nervous system as well as prevent cornea pathology and preserve the function of the visual axis. In conclusion, the humoral immune response elicited by prophylactic vaccines is a critical component of providing resistance to subsequent HSV challenge reinforced in this study and others[49,72]. In the human patient, it has been noted HSV-1-specific memory B cells including class-switched memory B cells are correlated with asymptomatic HSV-1 seropositive individuals in comparison to symptomatic HSV-1 seropositive patients underscoring the likely contribution of humoral immunity in HSV-1 surveillance in the latent-infected human host[73].

Materials and methods

Mice. Six-to-eight-week-old male and female C57BL/6 mice were obtained from Jackson Laboratory (Bar Harbor, ME) and housed under specific-pathogen free conditions in the animal vivarium at the Dean McGee Eye Institute. All procedures described under the methods section were approved by the University of Oklahoma Health Sciences Center animal care and use committee (protocol # 19–060 ACHIX). This study was carried out in compliance with the ARRIVE Essential 10 Guidelines.

Mice infection/vaccination. Animals were vaccinated with parental GFP105 or live-attenuated 0ΔNLS HSV-1 derived from KOS strain[5]. Briefly, mice were footpad injected with 1×10^5 PFU of GFP105 or HSV-1 0ΔNLS in 10ul of PBS. HSV-1 GFP105 has a GFP coding sequence on the immediate early ICP0 gene between codons 104 and 105 on exon 2 under a cytomegalovirus promoter, whereas HSV-1 0ΔNLS lacks the nuclear localization signal (NLS) motif, R-P-R-K-R-R, encoded by amino acids 501 to 508 on exon 3 on the GFP105 background. For tissue collection, mice were anesthetized by i.p. injection of ketamine and xylazine and blood collected prior to exsanguination. Alternatively, at day 21 post primary footpad immunization, anesthetized mice were immunized a second time in the ipsilateral flank (ID) with the same amount of virus described above. Thirty days post-booster, mice were anesthetized by i.p. injection of ketamine and xylazine and blood collected prior to exsanguination. The PLN and spleen were processed, and cells labeled as described below. Serum was fractionated using Microtainer serum separator tubes (Becton Dickinson, Franklin Lakes, NJ) and stored at −80 °C until used in serum immunoassays.

IL-21 cytokine measurement. IL-21 cytokine content in tissue was performed with a commercially available pre-coated IL-21 ELISA kit plate (Thermo Fisher Scientific, Waltham, MA USA). PLN harvested at day 7 post infection were placed into 1.5 mL snap-capped Eppendorf tubes (Advanced Bullet Blender, Troy, NY) containing RIPA buffer (50 mM Tris–HCl, 1% NP-40, 150 mM NaCl, 1 mM EDTA, and protease and phosphatase inhibitors) and then homogenized using a Bullet Blender Storm 24 (Advanced Bullet Blender). The samples were then centrifuged (10,000 × g, 1 min), and cell-free lysates were collected and frozen at −80 °C until analyzed in the IL-21 ELISA assay. Intracellular cytokine staining within $CD4^+$ T_{FH} cells was performed using a commercially available anti-mouse IL-21 antibody conjugated with PE (R&D Systems, Minneapolis, MN USA). Specifically, the lymph nodes collected at day 7 post-vaccination were passed through a 40 µm filter cell strainer (Midsci, St. Louis, MO) resulting in single-cell suspensions. Next, 3×10^6 cells were stimulated with phorbol 12-myristate 13-acetate (PMA, 100 nM) and ionomycin (1ug/ml) for 6 h in the presence of brefeldin A (GolgiPlug, BD Biosciences). After the incubation period, cells were washed and stained with an antibody cocktail (containing anti-mouse CD45 conjugated with PerCP-Cy5.5, anti-mouse CD3 conjugated with PE-Cy7, anti-mouse CD4 conjugated with APC-Cy7, anti-mouse CXCR5 conjugated with BV421, and anti-mouse PD-1 conjugated with FITC) for 15 min at room temperature. Next, the cells were fixed, permeabilized, and stained with anti-mouse IL-21 conjugated with PE. The samples were then acquired with a MacsQuant flow cytometer (Miltenyi Biotec, Bergisch Gladbach, Germany) and analyzed with FlowJo software (BD Biosciences, Medford, OR).

Isotype ELISA. IgG1 and IgG2b-specific HSV-1 antibody titers were measured by ELISA. Briefly, 96-well microtiter plates were coated with purified HSV-1 virions in carbonate buffer (pH 9.6) and incubated overnight at 37 °C. The plates were washed with PBS-polyoxyethylene (20) sorbitan monolaurate (Tween20, ThermoFisher Scientific, Waltham, MA) to remove excess antigen and serial dilutions of mouse sera were added to the wells followed by incubation at room temperature for 2 h. Next, the plates were washed with PBS-Tween and incubated with alkaline phosphatase-conjugated anti-mouse IgG1, or IgG2b detection antibodies (1:2000 dilution; Southern Biotechnology, Birmingham, AL) for 2 h at room temperature. Finally, the plates were washed with PBS-Tween and incubated with para-nitrophenyl phosphate substrate for 18 h at 37 °C. The optical density at 450 nm was measured using a Clariostar microplate reader (BMG Labtech, Ortenberg, Germany) with background correction at 540 nm.

Antibody neutralization assay. Antibody neutralization assays were performed by exposing the confluent monolayers (50,000 cells/well of 96-well microtiter plate) of Vero cells (American Type Culture Collection, Manassas, VA) to 10,000 PFU HSV-1 (McKrae strain) in the presence or absence of serial dilutions of serum in

the presence of guinea pig complement (Rockland Immunochemicals, Limerick, PA) for 2 h. Next, the serum dilutions were decanted, and Vero cells were incubated in RPMI 1640 medium supplemented with 10% heat-inactivated fetal bovine serum (FBS), 1 × antibiotic/antimycotic, and 10 µg/ml gentamicin (Gibco Life Technologies, Grand Island, NY) for 24 h. Neutralization titers were reported as the reciprocal serum dilution at which a 50% reduction in cytopathic effect is observed.

Flow cytometry. CD4 T_{FH} cells and B cell subpopulation characterization was assessed by flow cytometry at day 7 and day 21 post primary footpad immunization or 30 days post-booster. Briefly, spleens were passed through a 40 µm filter cell strainer (Midsci) resulting in single-cell suspensions followed by treatment with multispecies red cell lysis buffer (Thermo Fisher Scientific, Waltham, MA) for red cell removal. Next, cells were washed and resuspended in PBS supplemented with 2% FBS (herein referred to as staining buffer or SB). PLN were harvested at the indicated time points and processed identical to spleens. One million spleen- or PLN-derived cells were resuspended in 100ul of SB and stained for the following cell population: follicular $CD4^+$ T cells ($CD45^+CD3^+CD4^+PD\text{-}1^+CXCR5^+Bcl\text{-}6^+$), germinal B cells ($CD45^+CD19^+GL\text{-}7^+CD95^+$), plasma cells ($CD45^+B220^{low}CD138^+$), plasmablasts ($CD19^+CD138^+$) class-switched B cells ($CD45^+CD19^+IgM^-IgD^-$), subsets and effectors of regulatory B cells (Bregs): marginal zone B cells ($CD45^+CD19^+CD23^+CD21^-$) and B10 ($CD45^+CD19^+CD5^+CD1d^{high}$). The samples with stained cells were acquired with MacsQuant flow cytometer (Miltenyi Biotec) or spectral flow cytometer Aurora (Cytek Biosciences, Fremont, CA) as described previously[38]. For assessment of HSV-1 gB-specific $CD8^+$ T cell function, we utilized a procedure previously described by our group[74]. Acquired samples were exported as FCS files and further analyzed using FlowJo software version 10.8.1 (BD Biosciences, Medford, OR).

ELISPOT assay for evaluation IFN-γ. ELISPOT for IFN-γ was described previously[38]. Briefly, 96-plate with immobilon-P membrane were coated overnight with primary IFN-γ Ab (BD Biosciences). Cells isolated from spleen of mice harvested at day 21 and at day 30 after boost, were plated at concentration 5×10^5 cells per well followed by overnight re-stimulation with HSV-1 derived gB peptide, SSIEFARL (10 ug/ml). The plate was developed as described previously[38].

Visual axis assessment. Mechanosensory function, cornea edema and neovascularization, and visual acuity evaluations were performed by esthesiometry, optical coherence tomography, confocal microscopy, and optokinetic tracking responses as previously described[75].

Immunoprecipitation of HSV-1 proteins and identification by mass spectrometry. Sera obtained from GFP105- and 0ΔNLS-vaccinated mice collected 30 days post-boost were used to immunoprecipitate viral proteins from HSV-1-infected Vero cell lysates as previously described[50]. Tryptic digestion of isolated proteins and mass spectrometry analysis was performed as previously described[50].

Statistical analysis. Statistical analysis was performed using GraphPad Prism (version 9.3.0). Data were shown as means ± standard error of the mean (SEM). Each figure legend describes the statistical test used for data analysis. Differences comparing GFP105- to 0ΔNLS-vaccinated mice were considered significant with a p value < 0.05.

Data availability

The data sets generated and analyzed for this study are available from the corresponding author upon reasonable request.

Received: 1 June 2022; Accepted: 8 September 2022
Published online: 23 September 2022

References

1. Looker, K. J. *et al.* Global and regional estimates of prevalent and incident herpes simplex virus type 1 infections in 2012. *PLoS ONE* **10**, e0140765 (2015).
2. Chemaitelly, H., Nagelkerke, N., Omori, R. & Abu-Raddad, L. J. Characterizing herpes simplex virus type 1 and type 2 seroprevalence declines and epidemiological association in the United States. *PLoS ONE* **14**, e0214151 (2019).
3. Ayoub, H. H., Chemaitelly, H. & Abu-Raddad, L. J. Characterizing the transitioning epidemiology of herpes simplex virus type 1 in the USA: Model-based predictions. *BMC Med.* **17**, 57 (2019).
4. Itzhaki, R. F. Herpes simplex virus type 1 and Alzheimer's disease: possible mechanisms and signposts. *FASEB J.: Official Publication of the Federation of American Societies for Experimental Biology* **31**, 3216–3226 (2017).
5. Royer, D. J. *et al.* A highly efficacious herpes simplex virus 1 vaccine blocks viral pathogenesis and prevents corneal immunopathology via humoral immunity. *J. Virol.* **90**, 5514–5529 (2016).
6. Bloom, D. C., Tran, R. K., Feller, J. & Voellmy, R. Immunization by replication-competent controlled herpesvirus vectors. *J. Virol* **92**, e00616-18 (2018).
7. Srivastava, R. *et al.* Therapeutic mucosal vaccination of herpes simplex virus 2-infected guinea pigs with ribonucleotide reductase 2 (RR2) protein boosts antiviral neutralizing antibodies and local tissue-resident CD4(+) and CD8(+) TRM cells associated with protection against recurrent genital herpes. *J. Virol.* **93**, e02309-18 (2019).
8. Naidu, S. K. *et al.* Intramuscular vaccination of mice with the human herpes simplex virus type-1(HSV-1) VC2 vaccine, but not its parental strain HSV-1(F) confers full protection against lethal ocular HSV-1 (McKrae) pathogenesis. *PLoS ONE* **15**, e0228252 (2020).
9. Patel, C. D. *et al.* Trivalent glycoprotein subunit vaccine prevents neonatal herpes simplex virus mortality and morbidity. *J. Virol.* **94**, e02163-19 (2020).

10. Ramsey, N. L. M. *et al.* A single-cycle glycoprotein D deletion viral vaccine candidate, ΔgD-2, elicits polyfunctional antibodies that protect against ocular herpes simplex virus. *J. Virol.* **94**, e00335-20 (2020).
11. Corti, D. & Lanzavecchia, A. Broadly neutralizing antiviral antibodies. *Annu. Rev. Immunol.* **31**, 705–742 (2013).
12. Kado, R., Sanders, G. & McCune, W. J. Diagnostic and therapeutic considerations in patients with hypogammaglobulinemia after rituximab therapy. *Curr. Opin. Rheumatol.* **29**, 228–233 (2017).
13. Aksoy, S. *et al.* Rituximab-related viral infections in lymphoma patients. *Leuk Lymphoma* **48**, 1307–1312 (2007).
14. Kapoor, A. K., Nash, A. A. & Wildy, P. Pathogenesis of herpes simplex virus in B cell-suppressed mice: The relative roles of cell-mediated and humoral immunity. *J. Gen. Virol.* **61**(Pt l), 127–131 (1982).
15. Simmons, A. & Nash, A. A. Effect of B cell suppression on primary infection and reinfection of mice with herpes simplex virus. *J. Infect. Dis.* **155**, 649–654 (1987).
16. Beland, J. L., Sobel, R. A., Adler, H., Del-Pan, N. C. & Rimm, I. J. B cell-deficient mice have increased susceptibility to HSV-1 encephalomyelitis and mortality. *J. Neuroimmunol.* **94**, 122–126 (1999).
17. Deshpande, S. P., Kumaraguru, U. & Rouse, B. T. Dual role of B cells in mediating innate and acquired immunity to herpes simplex virus infections. *Cell Immunol.* **202**, 79–87 (2000).
18. Mesin, L., Ersching, J. & Victora, G. D. Germinal center B cell dynamics. *Immunity* **45**, 471–482 (2016).
19. Bannard, O. & Cyster, J. G. Germinal centers: Programmed for affinity maturation and antibody diversification. *Curr. Opin. Immunol.* **45**, 21–30 (2017).
20. Karrer, U. *et al.* On the key role of secondary lymphoid organs in antiviral immune responses studied in alymphoplastic (aly/aly) and spleenless (Hox11(-)/-) mutant mice. *J. Exp. Med.* **185**, 2157–2170 (1997).
21. Brinkmann, V., Geiger, T., Alkan, S. & Heusser, C. H. Interferon alpha increases the frequency of interferon gamma-producing human CD4+ T cells. *J. Exp. Med.* **178**, 1655–1663 (1993).
22. Farrar, J. D. *et al.* Selective loss of type I interferon-induced STAT4 activation caused by a minisatellite insertion in mouse Stat2. *Nat. Immunol.* **1**, 65–69 (2000).
23. Bryant-Hudson, K. M. *et al.* HSV-1 targets lymphatic vessels in the eye and draining lymph node of mice leading to edema in the absence of a functional type I interferon response. *Am. J. Pathol.* **183**, 1233–1242 (2013).
24. Fallet, B. *et al.* Interferon-driven deletion of antiviral B cells at the onset of chronic infection. *Sci. Immunol.* **1**, e6817 (2016).
25. Royer, D. J., Carr, M. M., Chucair-Elliott, A. J., Halford, W. P. & Carr, D. J. Impact of type I interferon on the safety and immunogenicity of an experimental live-attenuated herpes simplex virus 1 vaccine in mice. *J. virol.* **91**, e02342-16 (2017).
26. Royer, D. J. *et al.* Vaccine-induced antibodies target sequestered viral antigens to prevent ocular HSV-1 pathogenesis, preserve vision, and preempt productive neuronal infection. *Mucosal Immunol.* **12**, 827–839 (2019).
27. Pereira, J. P., Kelly, L. M. & Cyster, J. G. Finding the right niche: B-cell migration in the early phases of T-dependent antibody responses. *Int Immunol* **22**, 413–419 (2010).
28. De Silva, N. S. & Klein, U. Dynamics of B cells in germinal centres. *Nat. Rev. Immunol.* **15**, 137–148 (2015).
29. Hale, J. S. *et al.* Distinct memory CD4+ T cells with commitment to T follicular helper- and T helper 1-cell lineages are generated after acute viral infection. *Immunity* **38**, 805–817 (2013).
30. Vinuesa, C. G., Linterman, M. A., Yu, D. & MacLennan, I. C. Follicular helper T Cells. *Annu. Rev. Immunol.* **34**, 335–368 (2016).
31. Nutt, S. L., Hodgkin, P. D., Tarlinton, D. M. & Corcoran, L. M. The generation of antibody-secreting plasma cells. *Nat. Rev. Immunol.* **15**, 160–171 (2015).
32. Lam, W. Y. *et al.* Mitochondrial pyruvate import promotes long-term survival of antibody-secreting plasma cells. *Immunity* **45**, 60–73 (2016).
33. Lam, W. Y. *et al.* Metabolic and transcriptional modules independently diversify plasma cell lifespan and function. *Cell Rep.* **24**, 2479-2492.e2476 (2018).
34. Cantor, J. *et al.* CD98hc facilitates B cell proliferation and adaptive humoral immunity. *Nat. Immunol.* **10**, 412–419 (2009).
35. Rosser, E. C. & Mauri, C. Regulatory B cells: Origin, phenotype, and function. *Immunity* **42**, 607–612 (2015).
36. Yanaba, K. *et al.* A regulatory B cell subset with a unique CD1dhiCD5+ phenotype controls T cell-dependent inflammatory responses. *Immunity* **28**, 639–650 (2008).
37. Bankoti, R., Gupta, K., Levchenko, A. & Stäger, S. Marginal zone B cells regulate antigen-specific T cell responses during infection. *J. Immunol. (Baltimore, Md.: 1950)* **188**, 3961–3971 (2012).
38. Gmyrek, G. B., Predki, P., Gershburg, E. & Carr, D. J. J. Noncognate signals drive enhanced effector CD8(+) T cell responses through an IFNAR1-dependent pathway after infection with the prototypic vaccine, 0ΔNLS, against herpes simplex virus 1. *J. Virol.* **96**, e0172421 (2022).
39. Yun, H., Rowe, A. M., Lathrop, K. L., Harvey, S. A. & Hendricks, R. L. Reversible nerve damage and corneal pathology in murine herpes simplex stromal keratitis. *J. Virol.* **88**, 7870–7880 (2014).
40. Chucair-Elliott, A. J., Zheng, M. & Carr, D. J. Degeneration and regeneration of corneal nerves in response to HSV-1 infection. *Invest. Ophthalmol. Vis. Sci.* **56**, 1097–1107 (2015).
41. Filiberti, A., Gmyrek, G. B., Montgomery, M. L., Sallack, R. & Carr, D. J. J. Loss of osteopontin expression reduces HSV-1-induced corneal opacity. *Invest. Ophthalmol. Vis. Sci.* **61**, 24 (2020).
42. Rao, P. & Suvas, S. Development of inflammatory hypoxia and prevalence of glycolytic metabolism in progressing herpes stromal keratitis lesions. *J. Immunol. (Baltimore, Md.: 1950)* **202**, 514–526 (2019).
43. Twardy, B. S., Channappanavar, R. & Suvas, S. Substance P in the corneal stroma regulates the severity of herpetic stromal keratitis lesions. *Invest. Ophthalmol. Vis. Sci.* **52**, 8604–8613 (2011).
44. Thomas, J., Gangappa, S., Kanangat, S. & Rouse, B. T. On the essential involvement of neutrophils in the immunopathologic disease: Herpetic stromal keratitis. *J. Immunol. (Baltimore, Md.: 1950)* **158**, 1383–1391 (1997).
45. Gimenez, F., Suryawanshi, A. & Rouse, B. T. Pathogenesis of herpes stromal keratitis–a focus on corneal neovascularization. *Prog. Retin. Eye Res.* **33**, 1–9 (2013).
46. Wuest, T., Zheng, M., Efstathiou, S., Halford, W. P. & Carr, D. J. The herpes simplex virus-1 transactivator infected cell protein-4 drives VEGF-A dependent neovascularization. *PLoS Pathog.* **7**, e1002278 (2011).
47. Hendricks, R. L., Tumpey, T. M. & Finnegan, A. IFN-gamma and IL-2 are protective in the skin but pathologic in the corneas of HSV-1-infected mice. *J. Immunol. (Baltimore, Md.: 1950)* **149**, 3023–3028 (1992).
48. Gurung, H. R., Carr, M. M., Bryant, K., Chucair-Elliott, A. J. & Carr, D. J. Fibroblast growth factor-2 drives and maintains progressive corneal neovascularization following HSV-1 infection. *Mucosal. Immunol.* **11**, 172–185 (2018).
49. Awasthi, S. *et al.* Trivalent nucleoside-modified mRNA vaccine yields durable memory B cell protection against genital herpes in preclinical models. *J. Clin. Investig.* https://doi.org/10.1172/JCI152310 (2021).
50. Carr, D. J. J. *et al.* Distinguishing features of high- and low-dose vaccine against ocular HSV-1 infection correlates with recognition of specific HSV-1-encoded proteins. *Immunohorizons* **4**, 608–626 (2020).
51. Cattoretti, G. *et al.* BCL-6 protein is expressed in germinal-center B cells. *Blood* **86**, 45–53 (1995).
52. Muramatsu, M. *et al.* Class switch recombination and hypermutation require activation-induced cytidine deaminase (AID), a potential RNA editing enzyme. *Cell* **102**, 553–563 (2000).
53. Liu, Y. J., Grouard, G., de Bouteiller, O. & Banchereau, J. Follicular dendritic cells and germinal centers. *Int. Rev. Cytol.* **166**, 139–179 (1996).

54. Fayette, J. *et al.* Dendritic cells enhance the differentiation of naïve B cells into plasma cells in vitro. *Scand. J. Immunol.* **48**, 563–570 (1998).
55. Dubois, B. *et al.* Dendritic cells enhance growth and differentiation of CD40-activated B lymphocytes. *J. Exp. Med.* **185**, 941–951 (1997).
56. Johnson-Léger, C., Hasbold, J., Holman, M. & Klaus, G. G. The effects of IFN-gamma on CD40-mediated activation of B cells from X-linked immunodeficient or normal mice. *J. Immunol. (Baltimore, Md.: 1950)* **159**, 1150–1159 (1997).
57. Finkelman, F. D., Katona, I. M., Mosmann, T. R. & Coffman, R. L. IFN-gamma regulates the isotypes of Ig secreted during in vivo humoral immune responses. *J. Immunol. (Baltimore, Md.: 1950)* **140**, 1022–1027 (1988).
58. Braun, D., Caramalho, I. & Demengeot, J. IFN-alpha/beta enhances BCR-dependent B cell responses. *Int. Immunol.* **14**, 411–419 (2002).
59. Gujer, C. *et al.* IFN-α produced by human plasmacytoid dendritic cells enhances T cell-dependent naïve B cell differentiation. *J. Leukoc. Biol.* **89**, 811–821 (2011).
60. Dubois, B. *et al.* Critical role of IL-12 in dendritic cell-induced differentiation of naive B lymphocytes. *J. Immunol. (Baltimore, Md.: 1950)* **161**, 2223–2231 (1998).
61. Crotty, S. T follicular helper cell differentiation, function, and roles in disease. *Immunity* **41**, 529–542 (2014).
62. Qi, H. T follicular helper cells in space-time. *Nat. Rev. Immunol.* **16**, 612–625 (2016).
63. Rasheed, M. A. *et al.* Interleukin-21 is a critical cytokine for the generation of virus-specific long-lived plasma cells. *J. Virol.* **87**, 7737–7746 (2013).
64. Bessa, J., Kopf, M. & Bachmann, M. F. Cutting edge: IL-21 and TLR signaling regulate germinal center responses in a B cell-intrinsic manner. *J. Immunol. (Baltimore, Md.: 1950)* **184**, 4615–4619 (2010).
65. King, I. L., Mohrs, K. & Mohrs, M. A nonredundant role for IL-21 receptor signaling in plasma cell differentiation and protective type 2 immunity against gastrointestinal helminth infection. *J. Immunol. (Baltimore, Md.: 1950)* **185**, 6138–6145 (2010).
66. Linterman, M. A. *et al.* IL-21 acts directly on B cells to regulate Bcl-6 expression and germinal center responses. *J. Exp. Med.* **207**, 353–363 (2010).
67. Stanfield, B. A., Pahar, B., Chouljenko, V. N., Veazey, R. & Kousoulas, K. G. Vaccination of rhesus macaques with the live-attenuated HSV-1 vaccine VC2 stimulates the proliferation of mucosal T cells and germinal center responses resulting in sustained production of highly neutralizing antibodies. *Vaccine* **35**, 536–543 (2017).
68. Yang, K. *et al.* T cell-derived lymphotoxin is essential for the anti-herpes simplex virus 1 humoral immune response. *J. Virol.* **92**, e00428-18 (2018).
69. Akkaya, M. & Pierce, S. K. From zero to sixty and back to zero again: The metabolic life of B cells. *Curr. Opin. Immunol.* **57**, 1–7 (2019).
70. Egawa, T. & Bhattacharya, D. Regulation of metabolic supply and demand during B cell activation and subsequent differentiation. *Curr. Opin. Immunol.* **57**, 8–14 (2019).
71. Rowe, A. M. *et al.* Herpes keratitis. *Prog Retin Eye Res* **32**, 88–101 (2013).
72. Awasthi, S. *et al.* Nucleoside-modified mRNA encoding HSV-2 glycoproteins C, D, and E prevents clinical and subclinical genital herpes. *Sci. Immunol.* **4**, e7083 (2019).
73. Dhanushkodi, N. R. *et al.* Antiviral CD19(+)CD27(+) memory B cells are associated with protection from recurrent asymptomatic ocular herpesvirus infection. *J. Virol.* **96**, e0205721 (2022).
74. Gmyrek, G. B. *et al.* HSV-1 0ΔNLS Live-attenuated vaccine protects against ocular HSV-1 infection in the absence of neutralizing antibody in HSV-1 gB T cell receptor-specific transgenic mice. *J. Virol.* **94**, e01000-20 (2020).
75. Carr, D. J. J., Berube, A. & Gershburg, E. The durability of vaccine efficacy against ocular HSV-1 infection using ICP0 mutants 0ΔNLS and 0ΔRING Is lost over time. *Pathogens* **10**, 1470 (2021).

Acknowledgements

This work was supported by NIH/NIAID grant R01 AI053108, P20 GM103477, P30 EY021725 as well as an unrestricted grant from Research to Prevent Blindness.

Author contributions

The study was conceived by G.B.G. and D.J.J.C. The experimental design and experiments were performed by G.B.G., A.N.B., V.H.S., and D.J.J.C. The manuscript was written by G.B.G. and edited by D.J.J.C. All authors reviewed the manuscript.

Competing interests

D.J.J.C. is an unpaid consultant for the company, Rational Vaccines Inc., that owns the patent rights to the HSV-1 0ΔNLS vaccine. All other authors have no competing interests.

Additional information

Correspondence and requests for materials should be addressed to D.J.J.C.

Reprints and permissions information is available at www.nature.com/reprints.

Publisher's note Springer Nature remains neutral with regard to jurisdictional claims in published maps and institutional affiliations.